Supporting Information

Wu et al. 10.1073/pnas.0908837106

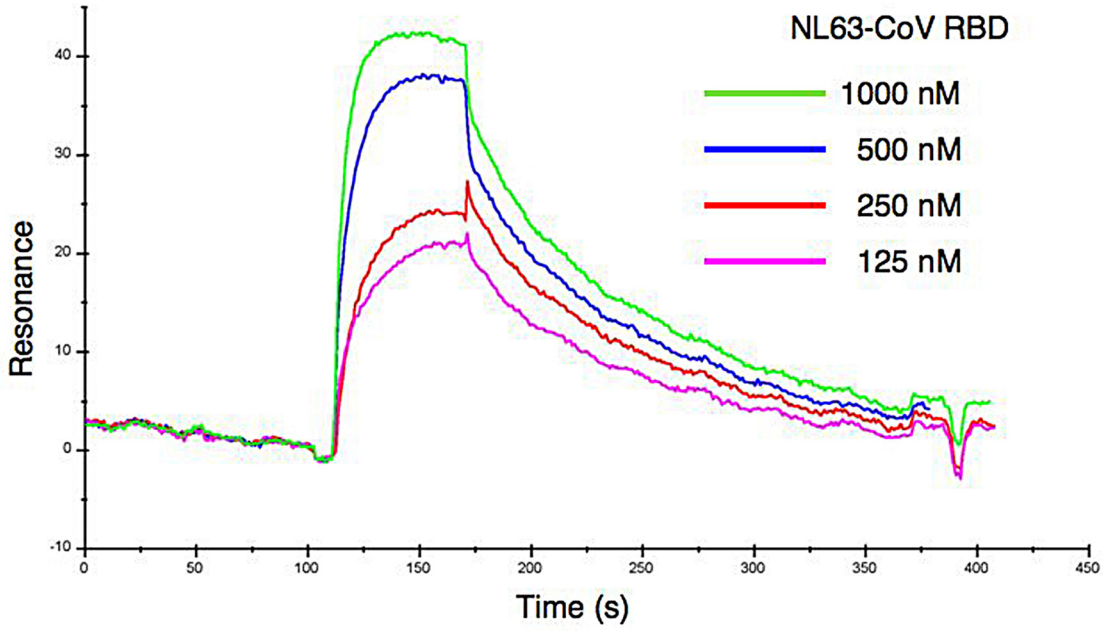

Fig. S1. Kinetics and binding affinity of NL63-CoV RBD and human ACE2 by surface plasmon resonance using Biacore. Human ACE2 was immobilized on a C5 sensor chip. NL63-CoV RBD was introduced at 20 μL/min at the indicated concentrations. Kinetic parameters were determined with BIA-EVALUATIONS software and are shown in Fig. 1*E*.

Fig. S2. Sequence alignment of NL63-CoV RBD with predicted RBDs of 4 other group I coronaviruses. The alignment was generated by the ClustalW program. RBMs are in red, 4 conserved cysteines in the core structure are in magenta, 2 cysteines existent in RBM1 of NL63-CoV but missing in other group I coronaviruses are in blue, and 2 cysteines existent in RBM2 of other group I coronaviruses but missing in NL63-CoV are also in blue. Beta-strands are drawn as arrows. The GenBank accession numbers are as follows: AAY16375 (FIPV), DQ112226 (CCoV), AAB30949 (TGEV), CAA42686 (PRCV), and CAA42686 (NL63). Asterisks indicate positions that have a single, fully conserved residue. Colons indicate positions that have strongly conserved residues. Periods indicate positions that have weakly conserved residues.

Table S1. Crystallographic data collection and refinement statistics

Data	
Space group	$P4_3$
Cell constants (Å, °)	a = 77.9, b = 77.9, c = 631.6
Resolution (Å)	50–3.3
Mosaicity (°)	0.6
R_{symm} (last shell)	13.5% (68.7%)
Observed (unique) reflections	236,281 (54,947)
Redundancy (last shell)	4.3 (4.2)
Completeness (last shell)	99.0% (98.5%)
I/s (last shell) 9.1 (2.6)	
Refinement	
R_{work} (R_{free})	27.6% (30.8%)
Correlation coefficent Fo-Fc	0.899
Correlation coefficent Fo-Fc (free)	0.873
R_{free} reflections	5%
<model B> (Å^2)	47.3
Bond lengths (Å) rms	0.014
Bond angles (°) rms	1.694
CHIRAL rms (Å^3)	0.125
Residues in each RBD	110
Residues in each ACE2	596
Glycans in each complex	9
Ramachandran plot	88.1% (core), 10.3% (allow), 1.6% (disallow)

Data were collected at $\lambda = 1.255$ Å at APS beamline 19 ID.

$R_{symm} = \Sigma_{i,h} | I_{i,h} - < I_h > | / \Sigma_{i,h} | I_{i,h} |$ where $< I_h >$ is the mean of the i observations of the reflection h.

$R_{work} = \Sigma||F_o| - |F_c|| / \Sigma |F_o|$. R_{free} is the same statistic, but calculated from a subset of the data (5%) that has not been used using refinement.

X-ray diffraction data were processed using HKL2000 (1). Program CCP4 AMoRe was used to find the molecular replacement solutions (2). Program CCP4 dmmulti was used for the electron density averaging (3). Program O was used for model building (4). Programs CNS (5) and CCP4 refmac (6) were used for structure refinement.

1. Otwinowski Z, Minor W. (1997) Processing of x-ray diffraction data collection in oscillation mode. *Methods Enzymol* 276:307–326.
2. Navaza J (2001) Implementation of molecular replacement in AMoRe. *Acta Crystallogr D Biol Crystallogr* 57(Pt 10):1367–1372.
3. Cowtan K (1994) dm: An automated procedure for phase improvement by density modification. *Joint CCP4 and ESF-EACBM Newsletter Protein Crystallogr* 31:34–38.
4. Jones TA, Zou JY, Cowan SW, Kjeldgaard (1991) Improved methods for building protein models in electron density maps and the location of errors in these models. *Acta Crystallogr A* 47(Pt 2):110–119.
5. Brunger AT, et al. (1998) Crystallography & NMR system: A new software suite for macromolecular structure determination. *Acta Crystallogr D Biol Crystallogr* 54(Pt 5):905–921.
6. Murshudov GN, Vagin AA, Lebedev A, Wilson KS, Dodson EJ (1999) Efficient anisotropic refinement of macromolecular structures using FFT. *Acta Crystallogr D Biol Crystallogr* 55(Pt 1):247–255.

Table S2. Summary of NL63-CoV RBD mutations that greatly affect protein expression or receptor binding (1, 2), and their locations in the structure

RBD residue	Mutation	Protein expression	Receptor binding	Location in the structure
Wild-type	None	High	High	Figs.1*B*, 2*C*
Cys497	C497A	High	None	RBM1
Tyr498	Y498H	High	None	RBM1
Val499	V499L	High	None	RBM1
Cys500	C500A	High	None	RBM1
Lys501	K501N	High	None	RBM1
Cys516	C516A	None	None	Strand 2b
Val531	V531E	High	None	RBM2
Gly534	G534A	High	None	RBM2
Gly537	G537R	High	None	RBM2
Asp538	D538A	High	None	RBM2
Ser540	S540N	High	None	RBM2
Cys550	C550A	None	None	Strand 4
Cys567	C567A	None	None	Strand 4b
Cys577	C577A	None	None	Strand 5
Glu582	E582N	High	None	RBM3
Trp585	W585R	High	None	RBM3

1. Li WH, et al. (2007) The S proteins of human coronavirus NL63 and severe acute respiratory syndrome coronavirus bind overlapping regions of ACE2. *Virology* 367:367–374.
2. Lin HX, et al. (2008) Identification of residues in the receptor-binding domain (RBD) of the spike protein of human coronavirus NL63 that are critical for the RBD-ACE2 receptor interaction. *J Gen Virol* 89:1015–1024.

Table S3. ACE2 residues that directly contact NL63-CoV or SARS-CoV

ACE2 residues that contact both viruses	ACE2 residues that contact NL63-CoV only	ACE2 residues that contact SARS-CoV only
H34, E37, Y41, Q325, N330, K353, G354	D30, N33, P321, N322, M323, T324, G326, D355, F356	Q24, T27, K31, D38, L45, L79, M82, Y83, Q325, E329